Electrical properties of single and multiple poly(3,4-ethylenedioxythiophene) nanowires for sensing nitric oxide gas

Hui-Hsin Lu[a], Chia-Yu Lin[b], Tzu-Chien Hsiao[c,d], Yueh-Yuan Fang[e], Kuo-Chuan Ho[b,f], Dongfang Yang[g], Chih-Kung Lee[h], Su-Ming Hsu[i], Chii-Wann Lin[a,e,h,*]

[a] Department of Electrical Engineering, National Taiwan University, Taipei, 10617, Taiwan
[b] Department of Chemical Engineering, National Taiwan University, Taipei, 10617, Taiwan
[c] Department of Computer Science, National Chiao Tung University, Hsinchu 30010, Taiwan
[d] Institute of Biomedical and Engineering, National Chiao Tung University, Hsinchu 30010, Taiwan
[e] Institute of Biomedical Engineering, National Taiwan University, Taipei 10617, Taiwan
[f] Institute of Polymer Science and Engineering, National Taiwan University, Taipei 10617, Taiwan
[g] Integrated Manufacturing Technologies Institute, National Research Council, London N6G 4X8, Canada
[h] Institute of Applied Mechanics, National Taiwan University, Taipei 10617, Taiwan
[i] Graduate Institute of Immunology, National Taiwan University, Taipei 10051, Taiwan

ARTICLE INFO

ABSTRACT

The electrical properties of conducting polymer, poly(3,4-ethylenedioxythiophene) (PEDOT), nanowires were studied to develop nitric oxide (NO) gas sensors with low working temperatures. A nanowire with a diameter of 300 nm was fabricated using dip-pen nanolithography (DPN) across a 55 μm gap between a pair of electrodes. The electrical properties of single or multiple PEDOT nanowires were examined by plotting the current–voltage (I–V) curves in the range −3 V to +3 V at temperatures between 298 K and 393 K. The conductance of parallel wires was normalized with respect to the dimensions of the fabricated nanowires. The single nanowire exhibited nonlinear conductance associated with hysteresis but multiple wires did not. The currents increased with the temperature and the I–V characteristics were consistent with the power law $G(T) \alpha T^{\alpha}$ with $\alpha \sim 5.14$ and 5.43. The responses to NO were highly linear and reproducible, indicating that sensing using PEDOT nanowires was reliable with a minimal concentration of NO of 10 ppm.

1. Introduction

The development of one-dimensional (1-D) nanostructures for applications in electronics, optics and sensors is a very active field of research. Progress in advanced fabrication approaches has led to the use of various materials to produce nanowires, including gold [1], platinum [2], silicon dioxide [3], titanium dioxide [4,5], conducting polymer (CP) [6,7] and even DNA [8]. Nanowires present numerous unique and interesting optical and electrical characteristics because of the quantum confinement transportation phenomena, which differ from those associated with continuous bands in bulk materials [9,10]. With respect to the electrical properties of nanowires, many investigations have studied single electron tunneling and various theories have been proposed to explain the electrical properties of nanowires [11–14]. Nanowires made of CP have drawn much research interest because of their advantages of ease of fabrication,

low cost, and, most importantly, wide range of tunable electrical properties.

CP can be easily formed in various forms from monomers in an aqueous environment by electrochemical synthesis. Single-step synthesis of biologically-functionalized nanowires by the incorporation of biological molecules during electrochemical polymerization has been performed [15]. Although electrochemical synthesis is a very feasible and convenient means of fabrication, the alignment of CP nanowire remains a challenge. Samitsu utilized "molecular combing" techniques to stretch poly(3,4-ethylenedioxythiophene) (PEDOT) nanowires on Pt nanoelectrodes [16] and Aleshin synthesized nanowires of helical polyacetylene in an asymmetric reaction field of chiral nematic liquid crystals [13,17]. Both groups proposed relatively easy approaches for fabricating CP nanowires. However, precisely aligning single and multiple CP nanowires across electrodes is difficult in both methods. The first approach also has the drawback that making consistent size of CP nanowires is difficult. Measurement of precise electrical parameters for further modeling analysis is important to the theoretical understanding of nanowire-based devices, such as single electron transistors (SET) and to sensing applications based on

---

* Corresponding author at: No. 1, Section 4, Roosevelt Road, Taipei 10617, Taiwan, ROC. Tel.: +886 2 33665272; fax: +886 2 33665268.
   E-mail address: cwlinx@ntu.edu.tw (C.-W. Lin).

nanostructures with finite sensing areas or volumes. This work reports on measurements made of direct-write PEDOT nanowires on gold electrodes by dip-pen nanolithography (DPN). The dimensions of nanopatterns can be easily controlled by varying the AFM tip size, the dwell time and environmental parameters, such as temperature and relative humidity. DPN offers many advantages over traditional microfabrications, such as flexibility of processing and fabrication procedures and the need for no photolithography[18].

For applications of gas sensors, the concentration of nitric oxide (NO) in the environment is an important index of air quality because of its potentially toxic effects. Current limits around the world on environmental NO gas levels are below 25 ppm [19]. Most available gas sensors are based on a metal oxide, semiconductor [20,21], or electrochemical sensing [22]. Many metal oxides, such as zinc oxide and tungsten trioxides, have been adopted to sense various gases. However, they function only at high working temperatures, such as above 200 °C, that allows the surface electrons to react with ambient oxygen [23,24]. Thus, implementing these sensors in low-power-consumption portable devices is difficult. However, electrochemical sensing commonly requires calibration because the membrane and electrolyte deteriorate, and so are not practically convenient. Common causes of interference include variations in temperature, humidity, oxygen level and volatile organic compounds (VOCs) in the working environment [25], which factors can be optimized using the sensor array method. Furthermore, the long responses times associated with the molecular dynamics of adsorption and desorption, and the diffusion barrier in the bulk materials, are expected to be minimized using nanoscale materials. Hence, the use of CPs as sensing materials is attracting increasing interest in the field of gas sensing because of their low cost, ease of fabrication, and low working temperature. Such an approach has been demonstrated by several groups who have used macro-electrodes with a thick film configuration [25]. The stability and reproducibility drop as the number of measuring cycles increase.

To the best of the authors' knowledge, PEDOT sensing material in the form of nanowires is applied here for the first time to detect NO gas by direct-write DPN methods with the optimal concentration of PEDOT ink. The nonlinear I–V characteristics of PEDOT nanowires at various temperatures (from room-temperature to 393 K) are obtained to compare the electrical properties of a single nanowire with those of multiple nanowires. Then, the three NO concentrations in a steady state were measured to calculate a calibration curve. Finally, the dynamic response of the NO sensor was measured and its stability and reproducibility evaluated.

2. Materials and methods

2.1. Preparation of interdigitated microelectrodes

Two gold microelectrodes were prepared in this experiment. The first was produced by traditional photolithography with a 55 μm gap between the pair of electrodes. In short, the interdigitated microelectrode pattern was obtained by mask alignment, exposure, development, metal deposition and lift-off on a p-type wafer with a pre-deposited 250 nm-thick insulating silicon dioxide layer (Summit Tech., Taiwan). The second is a gold microelectrode with a 3 μm gap between the pair of electrodes used for patterning single PEDOT nanowire. This gap was made by electron beam lithography (Elionix. Co., Japan) to expose the resist on the glass substrate and then the same fabrication procedure was followed for the gold electrode. Before nanopatterning, the microelectrodes were treated with piranha solution (H_2SO_4:H_2O_2 (v:v) = 3:1) at 80 °C for 20 min and then rinsed in DI water. The surface was treated for 8 min in oxygen plasma cleaner (Harrick Plasma, NY, U.S.A.) to modify its surface such that it became hydrophilic before patterning [26,27].

Therefore, the substrate surface could become negatively charged, providing a static electrical force to cause the attachment of the conducting polymer. For the initial experiment, the silicon wafer (Summit Tech., Taiwan) was cut into small squares of area 1 cm^2, and then the same cleaning process was implemented before nanolithography.

2.2. Preparation for nanolithography

PEDOT with doped PSS (polystyrenesulfonate) was purchased from Bayer, Inc. and was concentrated before nanolithography. Contact mode AFM probes were obtained from NanoInk Inc. (type B, NanoInk, Inc. II., U.S.A.) with a spring constant of 0.016 N m^{-1}. The AFM probe was dipped into the concentrated PEDOT solution for 30 s to 40 s and then dried gently using nitrogen gas. The relative humidity in the working chamber was set between 50% RH and 60% RH at room-temperature. All the nanolithography was performed using an NSCRIPTORTM DPNWriter (Ver. 3.6.5, NanoInk, II., U.S.A.). The maximum patterning area for a single AFM probe was 80 μm by 80 μm. Sixty-eight PEDOT nanowires were made from two sets of 34 lines with a pitch of 2 μm within an area of 66 μm^2, to cover the gap of 55 μm between the microelectrodes. Following patterning, the scanning function of a lateral force microscope (LFM) was used to confirm the fabricated nanopatterns and the resultant images were analyzed using nanoRule^{++} software (Ver. 2.5, Pacific Nanotechnology, II. U.S.A.).

2.3. Measurement of electrical properties

I–V curves of multiple PEDOT nanowires on interdigitated microelectrode are acquired using a potentiostat (CHI 440, CH Instrument U.S.A.) with a sweep potential in the range of -3 V to $+3$ V and a sweep rate of 25 mV sec^{-1} at temperatures from room-temperature to 393 K in steps of 20 K. I–V curve of the single nanowire that was patterned on the microelectrode with 3 μm gap was measured using a picoammeter (Model 6487, Keithley, U.S.A.) with a sweep rate of 0.6 V sec^{-1} at room-temperature. A control program was developed using LabVIEW software (Ver. 8.2, National Instrument Corp. U.S.A) to transmit digital signals through a serial interface (RS-232) from a picoammeter to a computer.

2.4. NO gas sensing setup

The performance of the fabricated nanosensor was measured against various concentrations of NO gases (99.9995%, ShenYi Gas Co., Taiwan) in a closed glass gas chamber with a constant flow rate of 250 mL min^{-1} [28]. The dynamic responses of PEDOT nanowires to repetitive NO–N_2 cycles were measured in amperometric mode by applying -10 V across the microelectrodes; the measurements were recorded using the same potentiostat as for the determination of the I–V curves.

3. Results and discussion

3.1. Fabrication and confirmation of performance of PEDOT nanowires

DPN is a method direct-write nanolithography that is implemented using an AFM probe with a nanometer spatial resolution. Therefore, ensuring the smoothness of the surface of the substrate is very important. Silicon wafer was adopted herein because of the inherent perfect lattices of its surface. Other than roughness, the hydrophobicity of the surface crucially determines the performance of nanolithography, especially when aqueous PEDOT is used. Normally, the surface of silicon forms a thin layer of silicon dioxide in air.
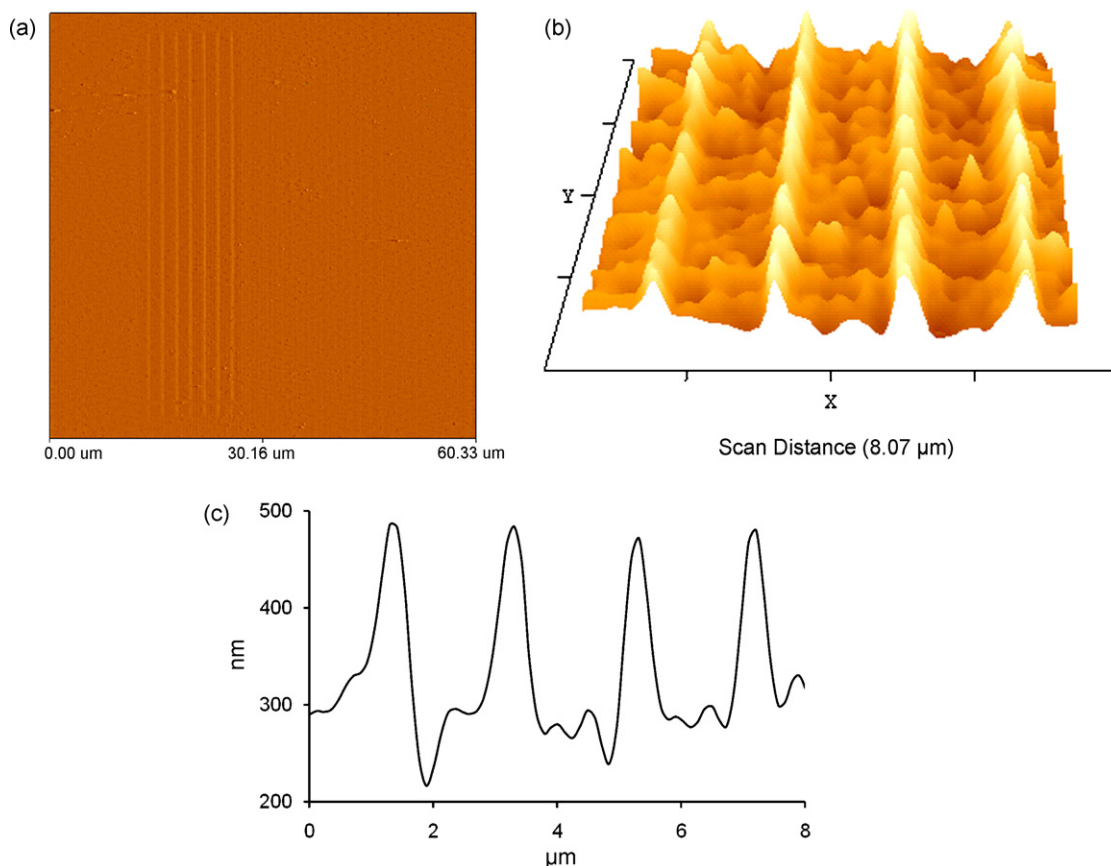
Fig. 1. (a) LFM image of PEDOT nanowires with measured line width of 240 nm and length of 52 μm on the surface of silicon wafer; (b) 3D image of fabricated nanowires with a 2 μm per unit scale on the along the x and y axes; (c) corresponding line profile to show the height of fabricated nanowires, which is approximately 200 nm.

The wafer can be soaked in piranha solution to remove this protective layer and then placed in an oxygen plasma cleaner to modify its surface properties. It thus becomes a hydroxyl-rich surface that has a weak electrostatic force for the attachment of PEDOT molecules in the DPN fabrication processes. Fig. 1(a) presents a lateral force microscopy (LFM) image of the resultant PEDOT nanowires. The nanowires were successfully patterned on the surface of a silicon wafer, and the width and length of these patterned nanowires were 240 nm and 52 μm, respectively. Accordingly, the aspect ratio of the PEDOT nanowires went as high as 200 times. As shown in Fig. 1 (b) and (c), the three dimensional images and line profiles of PEDOT nanowires are much clearer than the background of the substrate, and the height of nanowire was approximately 200 nm.

The interdigitated microelectrode was designed and fabricated on the silicon wafer, with a pre-deposited 250 nm-thick silicon dioxide layer to act as an insulation layer. The silicon wafer, with its native lattice surface, has an ultra-flat surface for DPN nanopatterning. Fig. 2(a) depicts the diagram interdigitated microelectrode. The electrical contact pads are in contact with the measurement system and the 1D nanopattern is written onto the space between the two adjacent electrodes. Fig. 2(b) presents part of the SEM image of the fabricated electrode; the light gray bands are the gold electrode
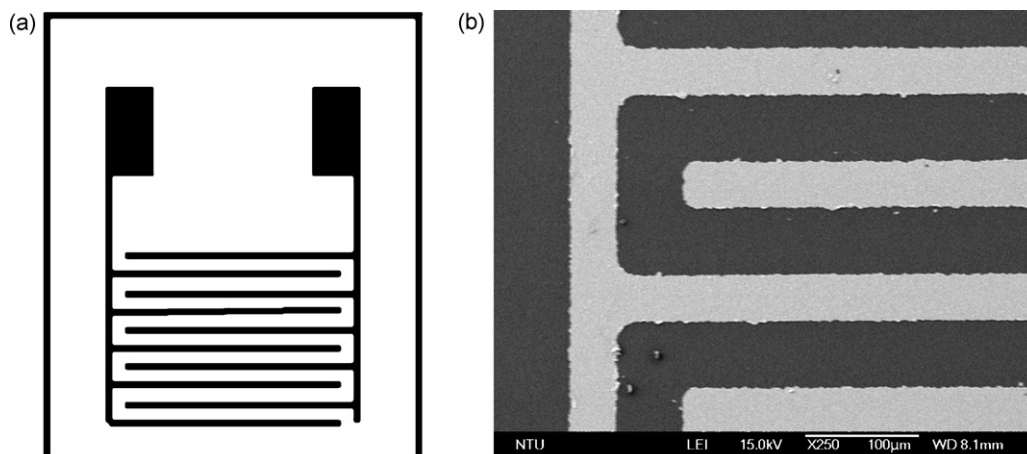
Fig. 2. (a) Schematic diagram of designed interdigitated microelectrode and (b) SEM image of fabricated device, where PEDOT nanowires are patterned by DPN across two horizontal gold electrodes.
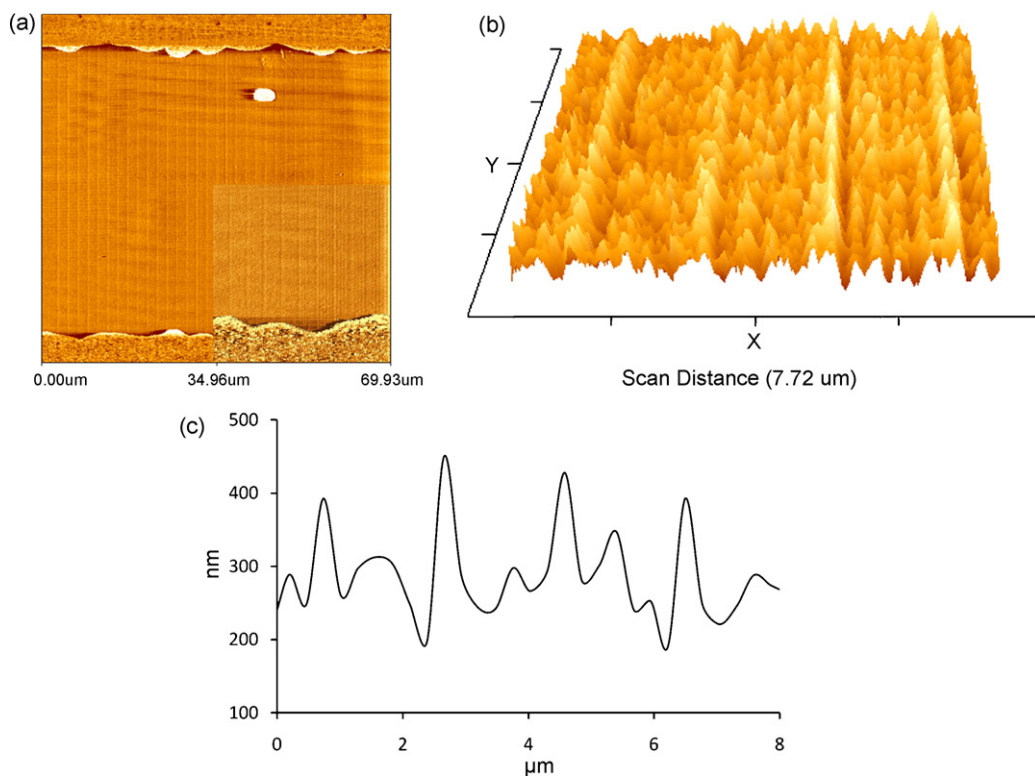
Fig. 3. (a) LFM image of 64 PEDOT nanowires, with 300 nm line width and 2 μm line pitch, between two Au electrodes; substrate is silicon wafer with pre-deposited 250 nm-thick layer of silicon dioxide for insulation. (Inset: enlargement of part of image to show more detail); (b) 3D surface image of fabricated nanowires with scale of 2.1 μm per unit along x and y axes; (c) corresponding line profile of scanned image; calculated mean difference between height of peaks and background is about 100 nm.

wires and the dark gray background is the silicon dioxide substrate. Fig. 3(a) shows an LFM image of the 68 lines of the PEDOT nanowires with a width of 300 nm and a line pitch of 2 μm, and gold microelectrodes on the upper and lower parts of the image. Fig. 3(b) shows a 3D plot of the fabricated nanowires with a rough background, which may be produced by the micro-fabrication process during the preparation of the microelectrode, as seen in Figs. 1 and 3, in which the native surface of the silicon wafer is smoother than the surface following the processes. However, the calculated mean difference between the peaks and the background is around 100 nm (Fig. 3(c)).

3.2. I–V characteristics

To determine the electrical properties of the fabricated PEDOT nanowires, their I–V curves were measured at various temperatures, from 298 K to 393 K, with an applied bias of −3 V and 3 V. The inset in Fig. 4(a) plots the background current with a bare electrode array at 393 K. The low background current (<nA) clearly indicates the effective insulation and the low leakage current between the electrodes and the substrate. The recorded currents are in the range of microAmperes, which is consistent with the electrical behavior of the patterned PEDOT nanowires. As shown in Fig. 4 (a), the recorded I–V curves exhibit nonlinear and asymmetric behavior. The structures of the fabricated devices can be viewed as an interface between metal (gold) and a p-type semiconductor (PEDOT:PSS). Hence, the conductivity in the reverse bias region exceeds that in the forward bias region. Restated, the potential barrier between the p-type semiconductor and the metal declines under the reverse bias, and the conductivity at the reverse bias exceeds that at forward bias. It also indicates that the temperature effect of PEDOT nanowires in stronger in the reverse bias region. These I–V curves demonstrate a positive correlation between recording current and the rising working temperature,

which is attributable to the increase in the kinetic energy of carriers within conducting polymer. Fig. 4(b) is a double log plot of the calculated conductance against temperature from 298 K to 393 K with applied constant biases of +3 V (solid triangles) and −3 V (solid squares). Aleshin et al. found that the conductance of conducting polymer nanofibers follows the power-law $G(T) \propto T^{\alpha}$ with the power exponent α in the range 2.2–7.7 [13,17]. According to the fitting results herein, the power exponent of α is 5.14 at forward bias and α is 5.43 at reverse bias, which results are consistent with published studies. The larger slope at a negative bias of −3 V is associated with higher sensitivity of conductance and nonlinear gains with increasing reverse biases for sensing applications.

A device with a single PEDOT nanowire in a 3 μm microelectrode that is at the lower limit of the proposed DPN system was prepared to compare its behavior with the measured nonlinear and asymmetrical behavior of multiple PEDOT nanowires. Fig. 4 (c) plots the I–V curve of a single PEDOT nanowire that was patterned across a 3 μm gold electrode gap by DPN. Since the recorded current in the single PEDOT nanowire is much lower than that in multiple nanowires, a picoameter was utilized to record the weak electrical signals. In the same bias range, the measured I–V curve of a single nanowire exhibited similar nonlinear and asymmetrical characteristics, without passing through the origin, perhaps because of changes in the induced dipole alignment as the applied electrical field crosses zero, increasing the contact barriers [29]. Hence, the I–V curve, exhibited hysteresis, does not pass through the origin with zero bias.

The dimensions of the PEDOT nanowires are another key factor that can influence their electrical behavior. The height of PEDOT nanowires cannot be measured from the brightness of the LFM images. Possible artifacts may arise because of the material properties of the specimen, the surface patterns and the spring constant of the used probe. The height of the fabricated patterns was calculated by assuming that the conductance per unit area of the cross section
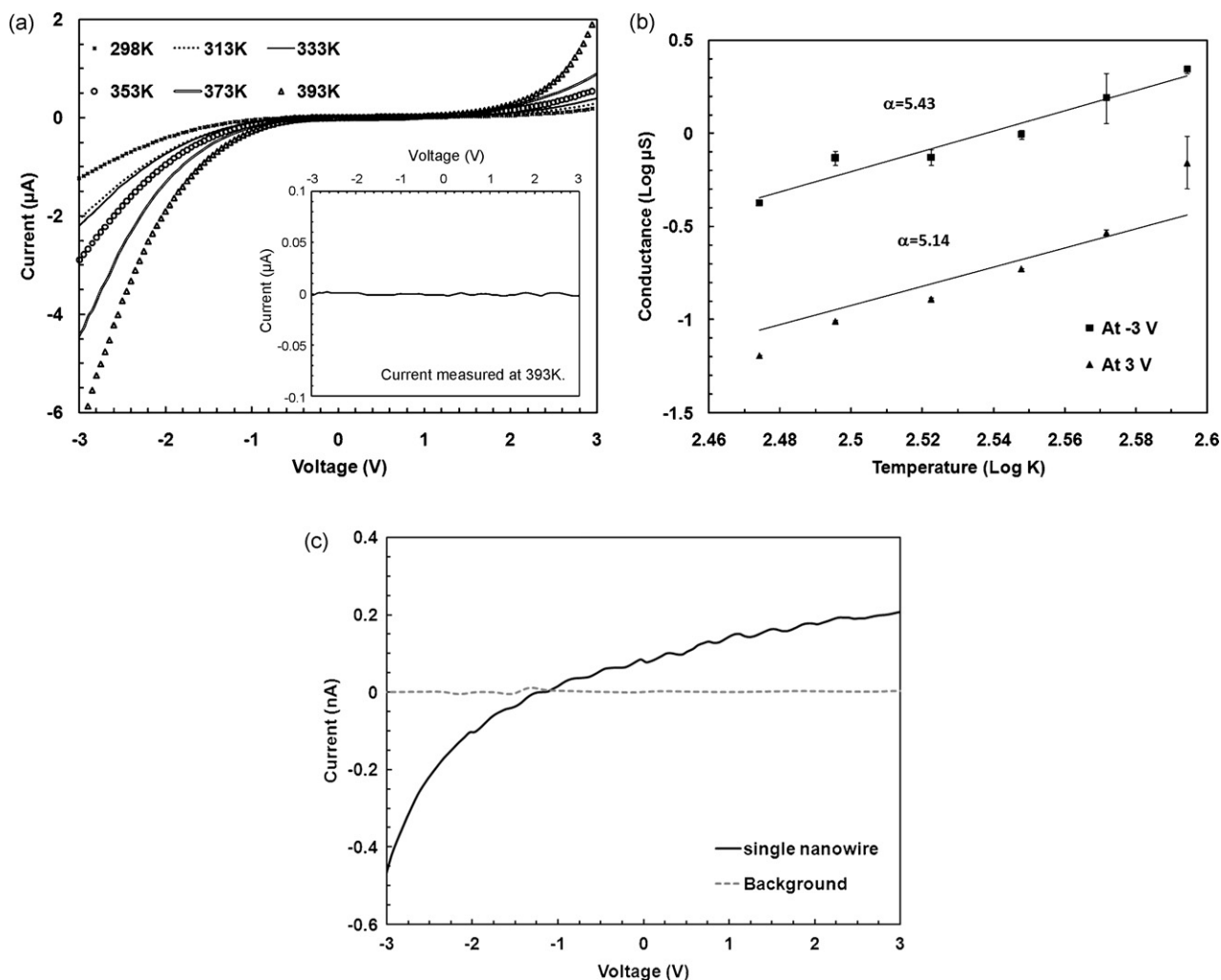
Fig. 4. (a) I–V curves of PEDOT nanowires at various temperatures from room-temperature to 393 K. Inset plots the voltage vs. current curve of bare microelectrode measured at 393 K. (b) Double log plot of calculated conductance (μS) against temperature (K) from 298 K to 393 K with constant biases of +3 V (solid triangle) and −3 V (solid square). (c) I–V curve of single PEDOT nanowire with length of 3 μm and width of 68 nm (solid) the dash line of background control.

was constant and that the heights of the PEDOT nanowires with widths of 300 nm and 68 nm are h_1 and h_2, respectively. Based on the results shown in Fig. 4 (a) and (c), the current at −3 V is 1.236 μA for 68 nanowires (with a width of 300 nm) and 0.467 nA for a single nanowire (with a width of 68 nm). The calculation yields 0.467 nA (current at −3 V) ÷[68 nm) × h_1 (*nm*)] = 1236 nA) (current at −3 V) ÷ [300 (nm)÷h_2 (nm) × 68 (lines)]). Hence, the ratio of h_1 to h_2 is 0.11. The height (h'_1) of the nanowire with a width of 300 nm in LFM (Fig. 1 (c)) is about 200 nm, and that (h'_2) of a single nanowire with a width of 68 nm in LFM (not show here) is about 20 nm, and thus the ratio of h'_1 to h'_2 is about 0.1, which is close to the result calculated from their electrical behaviors. The result indicates that the electrical behavior of 68 nanowires exhibits parallel connection, which can serve in the future as the basis of the design of a logic circuit.

3.3. Sensing gas

Based on the results in Fig. 4 (a), four working temperatures, 298 K, 313 K, 333 K and 353 K, were used in the NO gas sensing setup. The best working temperature in the current setup was about 353 K (80 °C) because of the detection limit of the potentiostat. Firstly, the steady-state measurement of I–V curves was performed to determine the performance of the PEDOT nanowires in various concentrations of NO. As presented in Fig. 5(a), the I–V curves measured in 0 ppm (solid line), 50 ppm (dashed line) and 100 ppm (cross line) NO gas over an extended bias range from −6 V to 0 V, respectively. The current passed in response to the 100 ppm NO gas exceeded that in response to the 50 ppm nitric oxide, indicating that the reaction of PEDOT nanowires with NO gas increases the concentration of carriers. One possible sensing mechanism is based on changes in electron density upon the physical adsorption/desorption of gas molecules by the PEDOTs. Several publications [28,30] have demonstrated that NO can react with sensing materials, such as carbon nanotubes, and thus increase their conductance by adding free electrons from defect sites. Flushing with nitrogen gas promotes desorption from the sensor surface and restores the baseline with less residual interference in the ambient environment. Moreover, the calculated sensitivity is approximately 1 μA ppm^{-1} at −6 V bias with good linearity ($y = -0.936x$) and correlation coefficient ($R^2 = 0.997$), as shown in Fig. 5(b). The estimated detection limit at S/N = 3 (signal-to-noise ratio = 3) is about 9 ppm. Fig. 5(c) plots the measured I–V curve in 10 ppm and the current difference is around 0.09 μA. This result demonstrates that the nanosensor made from PEDOT nanowires has the potential to sense the NO concentration in practical environmental applications due to the current limit, 25 ppm, of NO [19]. Moreover, the response is linear at applied biases of up to −10 V, as shown in the inset in Fig. 5 (a). The calculated sensitivity at −10 V against NO gas is approximately 1.6 μA ppm^{-1}. Therefore, a −10 V bias can be
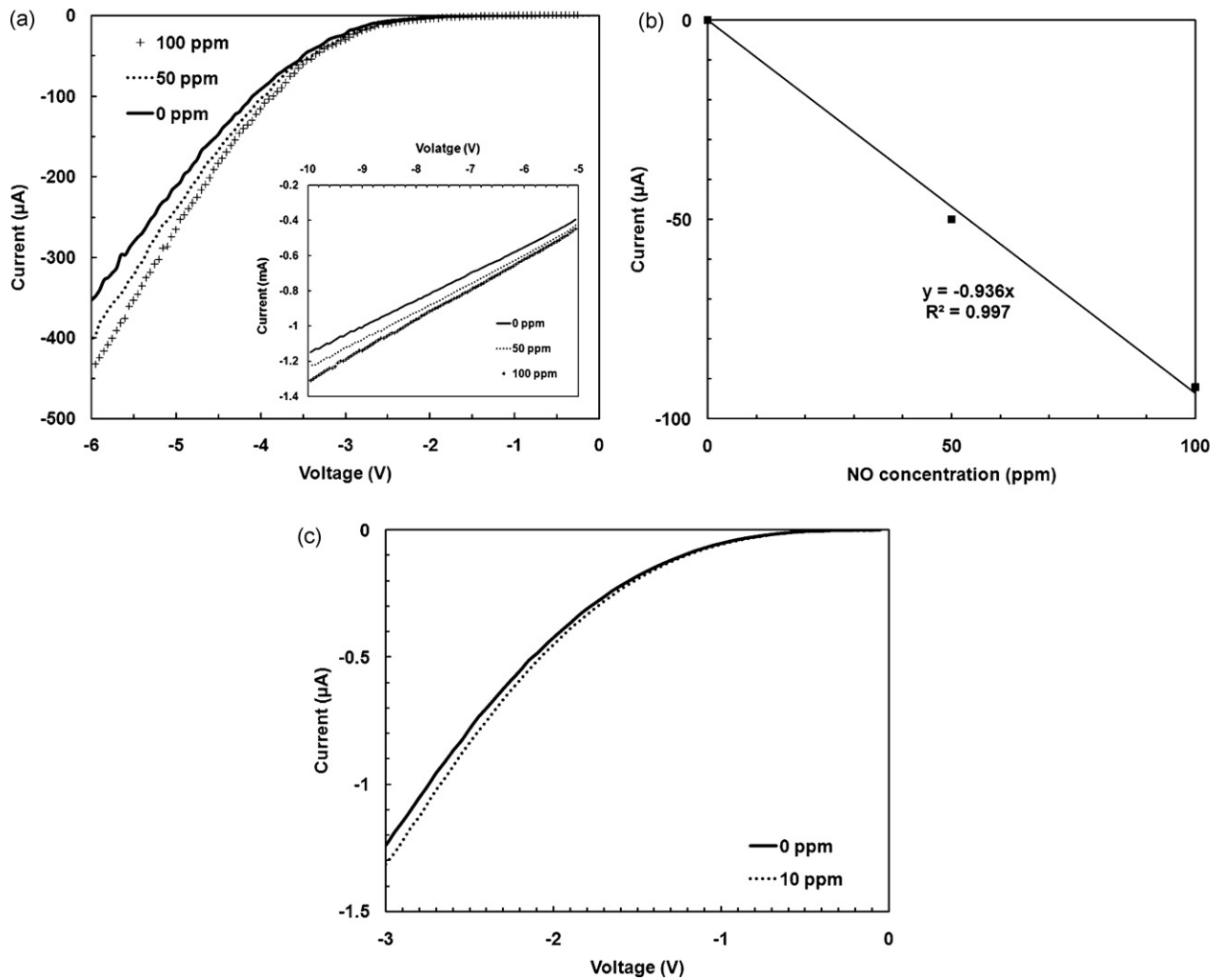
Fig. 5. (a) Measured *I–V* curves reveal performance of PEDOT nanowires in different concentrations of NO at 353 K with applied biases of 0 V and −6 V. Gas flow rate is 250 mL min^{-1} and the inset figure extends curve from −5 V to −10 V; (b) calculated sensitivity is approximately 1 μA ppm^{-1} at −6 V bias; linearity (y = −0.936x) and correlation coefficient (R^2 = 0.997) are favorable; (c) estimated detection limit at S/N = 3 is around 9 ppm.
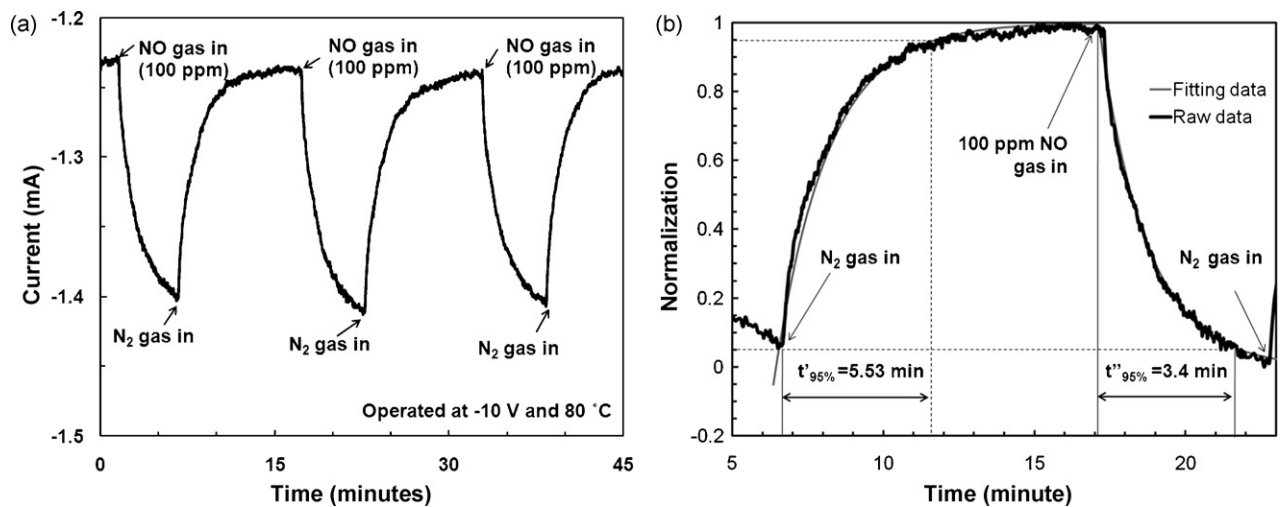
Fig. 6. (a) Current transient response of PEDOT nanowires-based sensor to 100 ppm NO gas, measured at bias of −10 V at 353 K (80 °C). Gas flow rate is 250 mL min^{-1}. (b) One of above figure three cycles. Black line represents raw data and gray line represents exponential fitting results.

applied to measure the dynamic response in the presence of NO gas.

Before the transient response of current to NO gas was measured, a continuous flow of nitrogen gas was used to pre-condition the sensor chip for a short period to eliminate the unwanted gas molecules to stabilize the background signal. Then, the NO gas was switched on and the conductivity of the PEDOT nanowires in the testing chamber therefore changed. When the current did not change for more than a minute, such that the response was quasi-stable, the NO gas channel was closed and the nitrogen (N_2) channel was opened to remove the residual NO. In our earlier studies of the responses of dip-coated thick-film PEDOT to NO, the baseline was restored after more than four hours [31]. In this work, the PEDOT nanowires took only about 11 min to recover to the baseline, which period is much less than four hours. Since the PEDOT nanowires made by DPN have a larger sensing surface and a thinner thickness, the sensing surface is expected to reach equilibrium more rapidly. Accordingly, this nanosensor provides better sensitivity than other film-type sensors and exhibits fast dynamics for practical applications. Fig. 6(a) displays the dynamic responses of PEDOT nanowires to exposure to 100 ppm NO and N_2 gases. The results show that this reproducible dynamic response is reversible. The signal-to-noise ratio in 100 ppm NO gas is quite high (SNR = 34), and the response times are about 15 min for adsorption and 10.83 min for recovery. The change in current caused by a reaction with 100 ppm NO gas is about 0.17 mA. The mean background current in nitrogen gas is about -1.23 ± 0.0049 mA ($n = 3$) and the mean current generated by 100 ppm NO is -1.40 ± 0.0158 mA ($n = 3$). Fig. 6 (b) plots a detailed analysis of one cycle of the dynamic response to determine the response time constants in NO and N_2 gases. A single exponential function was adopted to determine the optimal recovery, $t'_{95\%}$, and response time, $t'''_{95\%}$ plus $t'_{95\%}$, which is determined when the current reaches 95% of its final steady-state value. In Fig. 6(b), $t'_{95\%}$ is 5.5 min and $t''_{95\%}$ is 3.4 min, which values are two to three times better than those in our previous work [31], in which the response time was 10.3 min and the recovery time was 35.4 min.

The obtained results demonstrate that the PEDOT-based nanosensor exhibits good sensitivity and reproducibility and can be used for NO gas sensor applications. Although NO easily becomes NO_2 by reaction with oxygen in a typical environment, by NO and N_2 gases were mainly responsible for the changes in the currents in this work, because of isolation of the environmental oxygen by the sensing chamber. However, interference testing of various gases will be essential in the future to determine the selectivity of gas sensors based on PEDOT nanowires. The sensitivity can be further improved by increasing nanowire density and lowering working temperature. Therefore, the sensing and electrical properties of PEDOT nanowires will also be investigated further using DPN nanofabrication with a high spatial arrangement.

4. Conclusions

In summary, a gas nanosensor based on patterned PEDOT nanowires can be operated at a lower temperature than others sensors that are based on metal oxides. This work reports on the successful fabrication of PEDOT nanowires with a diameter of 300 nm in the gap between interdigitated microelectrodes by DPN. Experimental results demonstrated nonlinear electrical properties of multiple and single nanowires, whose conductance changed with temperature according to a power law with exponents of 5.14 (at 3 V) and 5.43 (at -3 V), respectively. The lowest NO concentration was 10 ppm in the present experimental setup, suggesting that good stability and good sensitivity make the PEDOT nanowire-based nanosensor a potential candidate for NO gas sensing applications.

Acknowledgments

References

[1] A. Correia, J.-L. Costa-Krämer, Y.W. Zhao, N. García, Nanostructured Materials 12 (1999) 1015–1020.
[2] G.-Y. Zhao, C.-L. Xu, D.-J. Guo, H. Li, H.-L. Li, Applied Surface Science. 253 (2007) 3242–3246.
[3] J.H. Kim, C.S. Yoon, Journal of Physical Chemistry C 112 (2008) 4463–4468.
[4] Y.X. Zhang, G.H. Li, Y.X. Jin, Y. Zhang, J. Zhang, L.D. Zhang, Chemical Physics Letters 365 (2002) 300–304.
[5] A.R. Armstrong, G. Armstrong, J. Canales, P.G. Bruce, Angewandte Chemie International Edition 43 (2004) 2286–2288.
[6] T. Thurn-Albrecht, J. Schotter, G.A. Kastle, N. Emley, T. Shibauchi, L. Krusin-Elbaum, K. Guarini, C.T. Black, M.T. Tuominen, T.P. Russell, Science 290 (2000) 2126–2129.
[7] S. Samitsu, T. Shimomura, K. Ito, M. Fujimori, S. Heike, T. Hashizume, Applied Physics Letters 86 (2005) 233103–1233103.
[8] Q. Gu, C. Cheng, R. Gonela, S. Suryanarayanan, S. Anabathula, K. Dai, D.T. Haynie, Nanotechnology 17 (2006) R14–R25.
[9] C. Pai-Chun, C. Chung-Jen, S. Daniel, R. Carsten, L. Jia Grace, Applied Physics Letters 90 (2007) 113101.
[10] X. Zhao, C.M. Wei, L. Yang, M.Y. Chou, Physical Review Letters 92 (2004) 236805.
[11] A. Rahman, M.K. Sanyal, Physical Review B (Condensed Matter and Materials Physics) 76 (2007) 045110–045116.
[12] D.Y. Vodolazov, F.M. Peeters, L. Piraux, S. Mátéfi-Tempfli, S. Michotte, Physical Review Letters 91 (2003) 157001.
[13] A.N. Aleshin, H.J. Lee, Y.W. Park, K. Akagi, Physical Review Letters 93 (2004) 196601.
[14] M.M. Fogler, S.V. Malinin, T. Nattermann, Physical Review Letters 97 (2006) 096601–096604.
[15] K. Ramanathan, M. Bangar, M. Yun, W. Chen, A. Mulchandani, N. Myung, Electroanalysis 19 (2007) 793–797.
[16] S. Samitsu, T. Shimomura, K. Ito, M. Fujimori, S. Heike, T. Hashizume, Applied Physics Letters 86 (2005) 233103.
[17] A.N. Aleshin, H.J. Lee, S.H. Jhang, H.S. Kim, K. Akagi, Y.W. Park, Physical Review B (Condensed Matter and Materials Physics) 72 (2005) 153202–153204.
[18] D.S. Ginger, H. Zhang, C.A. Mirkin, Angewandte Chemie International Edition 43 (2004) 30–45.
[19] K. Ashutosh, Current Opinion in Pulmonary Medicine 6 (2000) 21–25.
[20] G. Sberveglieri, W. Hellmich, G. Müller, Microsystem Technologies 3 (1997) 183–190.
[21] K.-D. Song, B.-S. Joo, N.-J. Choi, Y.-S. Lee, S.-M. Lee, J.-S. Huh, D.-D. Lee, Sensors and Actuators B: Chemical 102 (2004) 1–6.
[22] P.R. Warburton, M.P. Pagano, R. Hoover, M. Logman, K. Crytzer, Y.J. Warburton, Analytical. Chemistry 70 (1998) 998–1006.
[23] N. Yamazoe, N. Miura, Sensors and Actuators B: Chemical 20 (1994) 95–102.
[24] N. Koshizaki, T. Oyama, Sensors and Actuators B: Chemical 66 (2000) 119–121.
[25] H. Bai, G. Shi, Sensors 7 (2006) 267–307.
[26] J.-H. Lim, C.A. Mirkin, Advanced Materials 14 (2002) 1474–1477.
[27] S. Kooi, L. Baker, P. Sheehan, L. Whitman, Advanced Materials 16 (2004) 1013–1016.
[28] K.-C. Ho, Y.-H. Tsou, Sensors and Actuators B: Chemical. 77 (2001) 253–259.
[29] L. Yow-Jon, Journal of Applied Physics. 103 (2008) 063702.
[30] J. Mäklin, T. Mustonen, K. Kordás, S. Saukko, G. Tóth, J. Vähäkangas, Physica Status Solidi (b) 244 (2007) 4298–4302.
[31] H.-H. Lu, C.-Y. Lin, T.-C. Hsiao, K.-C. Ho, J. Tunney, D. Yang, S. Evoy, C.-K. Lee, C.-W. Lin, Engineering in Medicine and Biology Society, 2007, IEEE, Lyon, France, 2007.